Photophysical studies of CdTe quantum dots in the presence of a Zinc cationic porphyrin

Páraic M. Keane,[1] Shane A. Gallagher,[2] Luis M. Magno,[1] Miriam J. Leising,[1] Ian P. Clark,[3] Gregory M. Greetham,[3] Michael Towrie,[3] Yurii K. Gun'ko,[2]* John M. Kelly[2]* and Susan J. Quinn[1]*

The photophysical properties of 2.3 nm thioglycolic acid (TGA) coated **CdTe** quantum dots (QDs) prepared by a reflux method have been studied in the presence of a cationic meso-tetrakis(4-N-methylpyridyl) zinc porphyrin (**ZnTMPyP4**). Addition of the CdTe QDs to porphyrin in H_2O results in a marked red-shift and hypochromism in the porphyrin absorption spectrum, indicative of a non-covalent binding interaction with the QD surface. Low equivalents of the quantum dot were required for complete quenching of the porphyrin fluorescence revealing that one quantum dot may quench more than one porphyrin. Similarly addition of porphyrin to the quantum dot provided evidence for very efficient quenching of the CdTe photoluminescence, suggesting the formation of CdTe-porphyrin aggregates. Definitive evidence for such aggregates was gathered using small angle X-ray spectroscopy (SAXS). Ultrafast transient absorption data are consistent with very rapid photoinduced electron transfer (1.3 ps) and the resultant formation of a long-lived porphyrin species.

Introduction

Nano-sized quantum dots have attracted enormous interest due to their tuneable size, surface chemistry, and photophysical properties, which lead to numerous potential applications in photonics and biochemistry.[1] The II-VI metal chalcogenides such as ZnS, CdS, CdSe, CdTe, PbSe, and PbTe have been extensively studied and their variable direct band gap and resultant tuneable photoluminescence has led to numerous applications including photodynamic therapy, imaging and sensing applications.[2-11] Of particular interest is the use of quantum dots as acceptor/donor components for the conversion of light energy into electricity in a photovoltaic device.[12-16] A significant obstacle to the development of high-performance photovoltaic cells is the effective separation of photogenerated electron–hole pairs and the transfer of the electrons to the electrode. The interaction of luminescent organic photosensitisers with QDs in this way can lead to the construction of new light-harvesting photochemical and photoelectronic devices such as dye-sensitised solar cells (DSSCs), the properties of which are governed by excited-state dynamics at the molecule-QD interface.

To this end CdTe QDs are attractive candidates due to their relatively narrow band gap (~1.7 eV) and the emergence of routine aqueous based synthetic methods.[17] However, only a handful of studies have probed the charge and energy dynamics of CdTe QDs on the ultrafast timescale and even fewer have considered how these dynamics are influenced by the presence of suitable electron donor or acceptor surface species.[18-26] Due to the role in natural photosynthesis of related compounds porphyrin molecules have been extensively exploited for electron and energy transfer.[27-30] The light-harvesting properties of porphyrins has led them to be considered as components in solar photovoltaic cells.[31-34] Currently, bulk hetero junctions (BHJ) are considered to show most promise for improved solar cell efficiency. Recently, BHJs prepared from solution phase PbSe QDs and tetrabenzoporphyrin components were shown to be 40 times more efficient than a flat bilayer heterojunction (FHJ) comprising the same material.[35] A key aspect of the study of such photovoltaic systems is the nature of the interfacial charge dynamics between the porphyrin and the nanocomposite matrix, and how it contributes to the overall performance of the system. To consider this phenomenon we have studied the photophysical properties of a zinc porphyrin non-covalently assembled at the surface of uniform sized 2.3 nm CdTe QDs in water.

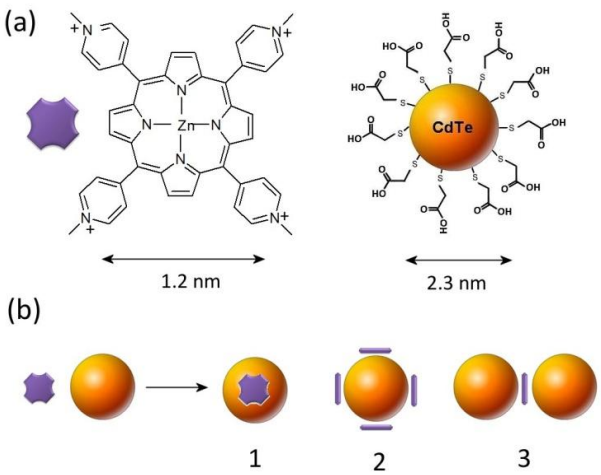

Scheme 1 Schematic representation of ZnTMPyP4 and CdTe systems

We believe this system is of interest as it affords the possibility to couple the high quantum yield efficiency of the QD to the electron/energy transport capabilities of an anchored porphyrin

molecule. The use of a porphyrin sensitising agent is advantageous as the UV-vis spectra of porphyrins (i) can be tuned by choice of central metal and (ii) are generally quite sensitive to binding interactions.[36-38] A number of systems based on non-covalent association of porphyrin molecules at a semiconductor surface have been prepared.[39-41] Recent work by Credi et. al. demonstrated energy transfer from a zinc phenylporphyrin non-covalently bound to 5.6 nm CdTe in chloroform evidenced by the presence of the soret band in the excitation spectrum of CdTe.[41] For this study the meso-tetrakis(4-N-methylpyridyl) zinc porphyrin, ZnTMPyP4 was chosen for its defined optical properties and water solubility. In addition the Zn metal centre results in a good separation between the porphyrin Soret band at 436 nm, and the exciton absorption band of the 2.3 nm CdTe QDs at 510 nm. Finally, the presence of four pyridinium residues with peripheral methyl substituents results in a positively charged porphyrin at neutral pH, which is expected to bind through electrostatic interactions to the negatively charged thioglycolic acid groups that passivate the surface of the CdTe, see Scheme 1.

The porphyrin and the QD may bind in different arrangements and some possible examples are schematically illustrated in Scheme 1. Study of the system using steady-state absorption and emission spectroscopy reveals a high affinity of the porphyrin for the QD surface which is accompanied by highly efficient quenching of the QD luminescence. The possible formation of small QD aggregates due to ZnTMPyP4 cross linking is considered by small angle X-ray scattering (SAXS). Finally, pump-probe transient absorption (TA) spectroscopy is used to profile the ultrafast processes that occur between the ZnTMPyP4 and CdTe QDs. Taken together this study reveals a system characterised by highly efficient transfer processes that further our understanding of energy and electron transfer at the quantum dot interface.

Results and Discussion

Steady State Spectroscopic Characterisation of ZnTMPyP4/CdTe QD assemblies

The absorption and emission spectra of the two separate components, ZnTMPyP4 and CdTe, are given in Fig. 1. At neutral pH the absorption spectrum of the ZnTMPyP4 is dominated by the intense and characteristic Soret band at 436 nm with two weaker Q-bands also present at 564 and 608 nm. Excitation of the porphyrin at 400 nm results in strong singlet emission between 600 and 750 nm (λ_{max} at 632 Q(0,0) and 666 nm Q(0,1)). The quantum yield of this emission is 2.5 %.[42] The steady state absorption spectrum of CdTe QDs in water shows a band at 510 nm, which is assigned to the first excitonic transition ($1s_e$-$1s_h$). Using this information the diameter of the QDs was determined spectroscopically to be 2.3 ± 0.2 nm.[43] This was corroborated using high resolution transmission electron microscopy (HRTEM), see ESI Fig. S1. The maximum number of COOH groups at the surface is estimated to be 75 when the surface footprint of a thiol group is taken to be 0.22 nm^2 and the surface area of a 2.3 nm diameter particle to be 16.6 nm^2.[44] Zeta-potential measurements (-48 mV) confirmed the presence of negatively charged COO^- surface groups at pH 7, see ESI Fig. S2.

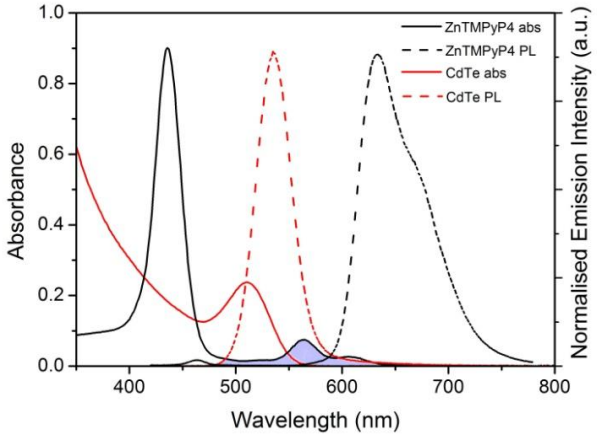

Fig.1 Comparison of the absorption spectra of equimolar concentrations of ZnTMPyP4 and CdTe (4.4 µM) in Millipore water and normalised emission spectra recorded upon excitation at 400 nm (note emission quantum yield for CdTe is approx. ten times greater than that of ZnTMPyP4).

The excitation of the QDs results in band edge photoluminescence centred at 535 nm with a quantum yield of 27%, calculated using the dye Rhodamine 6G as a reference. It is notable that the QD emission overlaps with the absorption of the porphyrin Q bands. This spectral overlap is indicated in Fig. 1 and may permit energy transfer from the QD to the porphyrin. By contrast energy transfer from the porphyrin to the QD is unlikely, both because of the energy disparity and the lack of overlap between the QD absorption in the region of 575 nm and the porphyrin emission.

Titration of **CdTe** QDs to a solution of **ZnTMPyP4**, (4.4 µM in Millipore water) resulted in a shift in the Soret band at 436 nm to 444 nm, which was accompanied by a dramatic decrease (>40%) in the absorbance. In addition, the Q-bands were found to shift from 564 and 608 nm to 573 and 616 nm respectively. Fig. 2 shows the changes to the porphyrin spectrum after the contribution of the QD absorption in the region has been subtracted (the raw data is given in ESI Fig. S3). Interestingly,

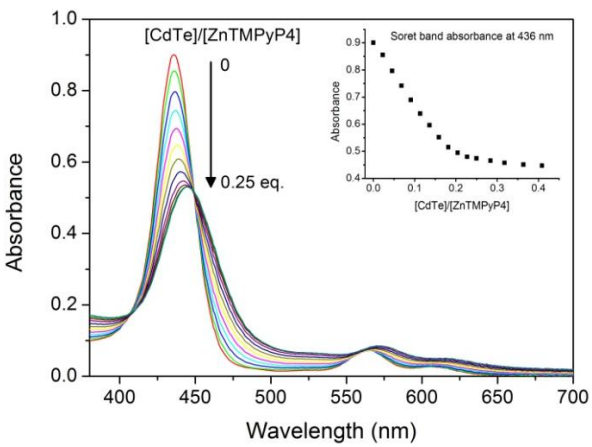

the changes in the porphyrin spectrum appear to reach completion upon addition of 0.4 equivalents of QDs (inset Fig. 2). Dramatic

Fig.2 UV/vis absorption spectra of 4.4 µM ZnTMPyP4 in the presence of increasing concentrations of CdTe (contribution of the CdTe absorbance to the spectra has been subtratcted). Inset: absorption at 434 nm plotted against CdTe equivalents.

changes occur between 0 and 0.25 equivalents of QDs and a clear isosbestic point is observed at 448 nm. This behaviour indicates that multiple ZnTMPyP4 binding events at the particle surface occur as independent events. These changes are similar to those previously observed for ZnTMPyP4 bound end-on to Quadruplex DNA.[38]

Next the interaction of ZnTMPyP4 and CdTe QDs was studied by monitoring the emission of the QD and porphyrin systems upon excitation at 400 nm where the solution remains essentially optically dilute (< 0.3) throughout the titration. The addition of QDs to an aqueous solution of ZnTMPyP4 resulted in a loss of ZnTMPyP4 emission at 635 nm with no concomitant shift in the position of fluorescence, see Fig. 3a. 95 % of the ZnTMPyP4 emission was quenched after the addition of only 0.25 QD equivalents, see inset Fig. 3a. This is in good agreement with the changes in the Soret band absorption in the UV-vis spectrum, inset Fig. 2. Furthermore, under these conditions no emission was detectable from the QDs. 99 % quenching of ZnTMPyP4 emission was observed upon the addition of 0.4 equivalents, after which the appearance of the QD emission at 554 nm was observed, see ESI Fig. S4. The emergence of QD emission at less than 1 equivalent signifies the association of more than one porphyrin per QDs already in solution. The same behaviour was observed upon excitation of the isosbestic point at 564 nm (see ESI Fig. S5) and is in excellent agreement with the behaviour observed for the UV/vis titration.

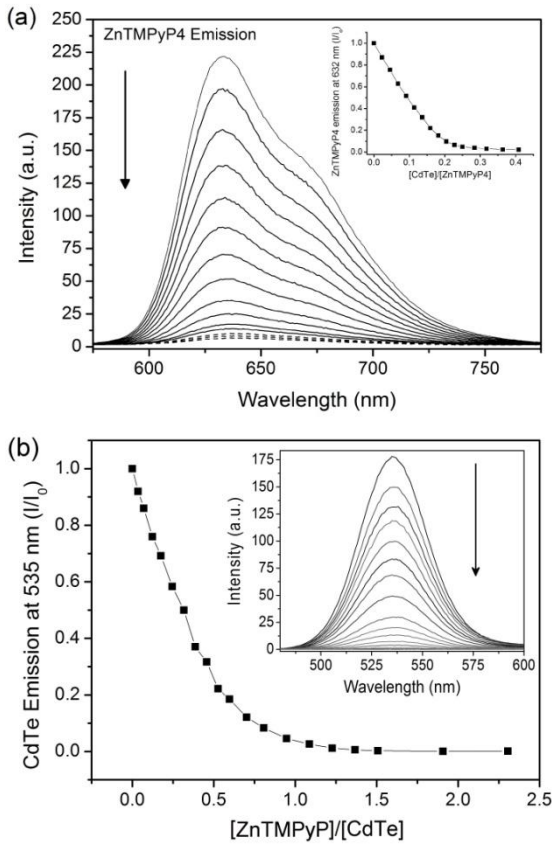

Fig.3 (a) Fluorescence spectra of 4.4 µM ZnTMPyP4 in presence of increasing CdTe (0-2.64 µM). λ_{exc} =400 nm. (b) PL of 2.5 µM CdTe in presence of increasing ZnTMPyP4 conc. (0 – 5.76 µM) and corresponding PL spectra (inset) . λ_{exc} = 400 nm.

The reverse titration was also conducted by adding the ZnTMPyP4 to the CdTe QDs. While the QD absorption was found to be largely unaffected, the position of the porphyrin bands were observed to be shifted to 444, 571 and 615 nm in the presence of the QDs which is in agreement with the observations above (see Fig. S6 ESI). In this case 96 % quenching of the QD emission was observed upon addition of one equivalent of the porphyrin with 99 % quenching observed after the addition of 1.5 equivalents of ZnTMPyP4, see Fig 3b.

The steady state absorption and emission results indicate the presence of discrete systems at different stoichiometric ratios of ZnTMPyP4 to CdTe QD. Dramatic changes are observed in the absorption and emission of ZnTMPyP4 upon addition of 0.25 QD equivalents which suggested that one QD is bound by four ZnTMPyP4 in solution. However, the end point of these titrations indicates that one QD is bound by on average two ZnTMPyP4s. The titration results compare favourably to those obtained by Uematsu et. al. who studied the emission quenching of CdTe by redox active species including methyl viologen and acridine.[46] This can be taken as an indication of the high binding affinity due to the presence of multiple charges on the ZnTMPyP4.

Small-Angle-Xray-Scattering (SAXS) of ZnTMPyP4 and CDTe QDs

The structure of the porphyrin:QD complexes formed in solution was investigated by small angle X-ray scattering (SAXS) under concentration conditions identical to the steady-state measurements. The scattering intensity has been used to calculate the pair distance distribution function (PDDF) p(q), which describes the paired-set of all distances between points within an object and is a Fourier inversion of the scattering curve calculated using a generalised indirect Fourier transformation (GIFT) technique.[47-49] This model has been used previously to account for rod-like assemblies of fullerenes in solution.[50] For particle aggregates the scattered light intensity is influenced by the structure present and such interparticle effects are typically represented by the structure factor S(q).[51,52] In the particular case of charged particles an additional approximation is necessary and the rescaled mean spherical approximation RMSA model (charged spheres model) has been applied here.[53, 54] The application of the RMSA model appears to be the most accurate model for the Porphyrin:QD complexes, see ESI note S1.

The PDDF data as a function of particle radius for the pure CdTe-TGA QDs in water is given in Fig. 4a. In the case of non-aggregated particles a single maximum in the PDDF is expected and observed.[55] The particle radius is extrapolated from the position of the peak maximum in the distribution curve (1.6 nm) and the maximum dimension (D_{max}) of the species is the value of r at p(r) = 0 which is obtained by extrapolation of the peak to the inflection point. In this case D_{max} = 3.8 nm which reveals that the particles have a slight ellipsoid shape (3.1 × 3.8 nm). In the presence of excess QDs to porphyrins (4:1) the particles remain essentially monodisperse and of similar size, see Fig. 4d. However, when the ratio of QDs to porphyrin is reduced to 2:1 the PDDF plot becomes structured with three distinct maxima now present. In the case of peak I D_{max} = 3.8 nm and reveals the presence of monomers. In the case of peaks II and III a D_{max} of 7.6 nm and 9.8 nm are observed, indicating the presence of dimers and trimers respectively, see Fig. 4b. The data is

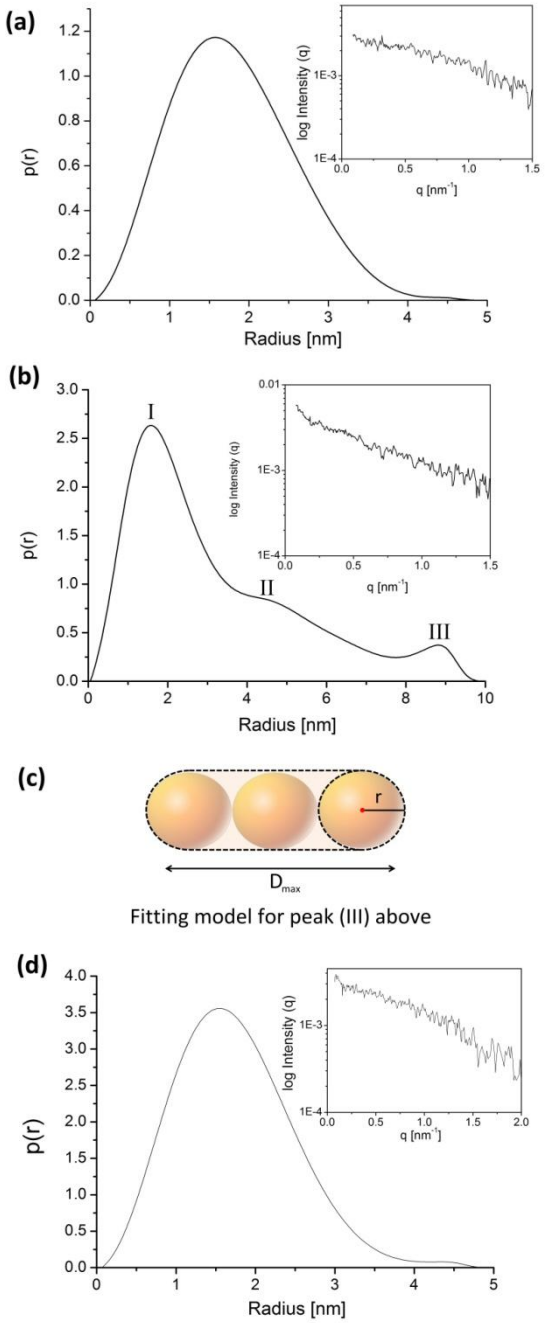

Fig. 4 A representative cross section PDDF, p(r), obtained from GIFT analysis of (a) CdTe QDs, (b) QD:ZnTMPyP4 (2:1), (c) Fitting model for peak (III) figure 4c. (d) QD:ZnTMPyP4 (4:1) in water.[QD] = 3.5 µM in all cases. Inset (Fig. 4a,b, d) SAXS experimental scattering curves.

consistent with the presence of linear aggregates represented by a cylinder with a cross-sectional radius r, see Figure 4c. Similar PDDF profiles have been observed for the in the case of streptavidin assembled gold trimers in solution.[55] Indeed even at 1:1 ratio of CdTe: ZnTMPyP4 the PDDF shows the presence of monomer species (ESI Fig. S7). Taken together the SAXS results indicate the presence of discrete systems at different stoichiometric ratios of ZnTMPyP4 to CdTe QD which reflects the different binding ratios indicated by the steady-state titrations.

Picosecond Transient Absorption

The efficient excited-state quenching, was further investigated by picosecond transient UV/vis absorption experiments by exciting at 400 nm (150 fs). Excitation of ZnTMPyP4 alone results in bleaching of the ground state at 437 nm and absorption at 480 nm, see Fig. 5a.[56] 90% of S_1 states (τ = 1.3 ns) then decay to the long-lived triplet state (τ = 2.8 µs, aerated solution).[42] This is reflected in the fact that the ground state does not recover over our longest recorded delay time of 3 ns and the transient absorption observed at 480 nm thus contains contributions from both S_1 and T_1.

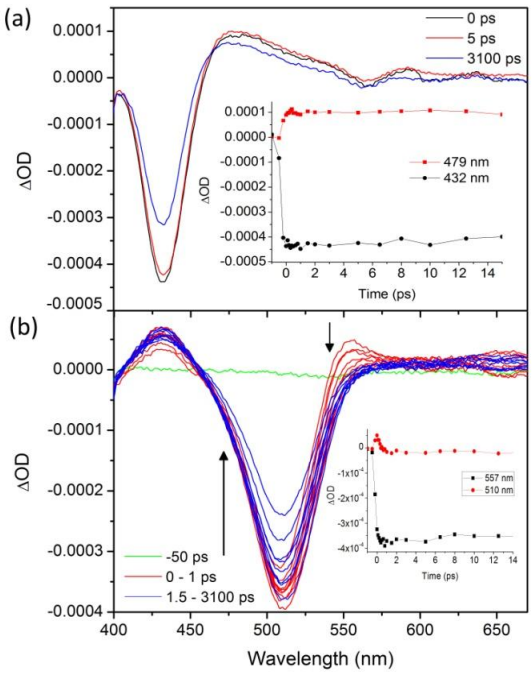

Fig. 5 (a) Ps Transient absorption of 5 µM **ZnTMPyP4** and (b) 5 µM **CdTe** in water. λ_{exc} = 400 nm, 25 nJ.

CdTe particles are known to be sensitive to multiphoton effects which result in exciton annihilation phenomena.[57] These events were minimised by the use of low laser energy (< 100 nJ). This energy regime was chosen based on results from a power dependence study, which indicated that experiments with laser power between 5-50 nJ were free from additional multi-photon events, see ESI Fig. S8. Excitation of the CdTe QDs at 400 nm under these conditions resulted in the rapid formation (within the response of the apparatus) of a strong bleach band in the band edge absorption at 510 nm, and the appearance of transient absorption bands at 431 and 554 nm, see Fig. 5b. The bleach was found to only partially recover (46 %) on the timescale of the experiment. This recovery was fit to a biexponential function to yield lifetimes of 15 ± 4 ps (10 %) and 3 ± 1 ns (36 %) (see ESI Fig S8). Notably the ground state of CdTe did not fully recover over the experiment timescale, consistent with the average photoluminescence lifetime being 13 ns. There is also a fast transient feature at 550 nm, which decays in less than 1 ps Fig. 5b.[57] The fact that this transient is also observed under conditions of low energy (5 nJ) suggests that this is not caused by multi-photon absorption.

Next the dynamics of CdTe /ZnTMPyP4 was investigated. A solution containing a 2:1 ratio of CdTe to ZnTMPyP4 was chosen to ensure the dominance of bound porphyrin {30% CdTe unbound (Fig. 3b)}. The extinction coefficient at 400 nm for CdTe is 70,000 and is estimated to be 20,000 M^{-1} cm^{-1} for bound ZnTMPyP4. Thus at 400 nm, for 2:1 QD: ZnTMPyP4, the relative absorption is 7:1 QD: ZnTMPyP4. Excitation of the sample using a laser energy of 10 nJ resulted in the instantaneous appearance of both the QD band edge bleach at 510 nm and the bound ZnTMPyP4 bleach at 445 nm (free porphyrin bleach occurs at 436 nm). Under these conditions it was possible to see the porphyrin bleach (445 nm) and transient (480 nm) and the QD bleach (510 nm).

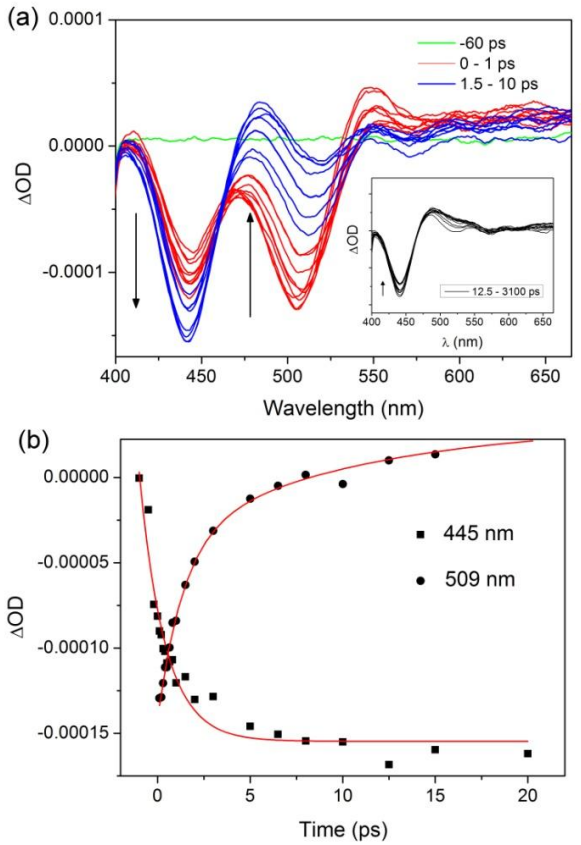

Fig. 6 Ps Transint absorption of 25 µM ZnTMPyP4 in presence of 50 µM CdTe (CdTe:ZnTMPyP4 = 2:1). λ_{exc} = 400 nm, 10 nJ.

On the 0 to 10 ps timescale the signal at 510 nm was found to recover almost completely (however this signal is a convolution of that of the transient porphyrin and of the bleach of the QD.) This recovery process coincided with a grow-in of the ZnTMPyP4 bleach at 445 nm, see Fig. 6. The grow-in of the porphyrin bleach can be adequately described by a single exponential fit of 1.3 ± 0.1 ps. The kinetics measured at 510 nm were found to be more complicated and were fitted using a bi-exponential function 1.3 ± 0.1 ps (60%) and 10.0 ± 2.6 ps (40%), see ESI Fig. S9. This is presumably due to contributions from more than one species. It was found that the decay phenomena were similar over the energy range 5-100 nJ (data recorded at 100 nJ excitation are also supplied in the see ESI Fig. S10 &S11). The porphyrin bleached state at 444 nm and transient at 480 nm are found to persist on the timescale of the experiment i.e. 3 ns. This suggests that a longer-lived porphyrin species, possibly the triplet, is formed from the quenched porphyrin. Interestingly, when the experiment was repeated at a 4:1 ratio of CdTe to ZnTMPyP4, a slower grow-in of the porphyrin bleach was observed, see ESI Fig. S12-S13. The recovery kinetics of the 510 nm bleach were similarly affected.

Energy and electron transfer are sensitive to the proximity of the species and the spectral overlap. If we assume binding occurs through electrostatic interactions between a ZnTMPyP4 (4+ charge) and multiple TGA-COO^- contacts then the donor-acceptor separation is only limited by the short TGA capping ligands. 400 nm light can excite both the porphyrin and QD. Thus a number of processes may give rise to the observed transient behaviour, see Scheme 2.

Case 1: Energy transfer from QD to porphyrin. There exists substantial overlap between the QD photoluminescence and the porphyrin Q-band absorption (shaded area in Fig. 1) and the process is also exergonic in nature. However, energy transfer from QDs to adjacent dye molecules would be expected to result in fluorescence enhancement of the dye (FRET)[58,59] as has been observed for related systems namely; from CdTe QDs in the presence of metal phthalocyanines.[60,61] No fluorescence from ZnTMPyP4 is observed in our experiments and thus this mechanism is discounted as the likely origin of the phenomena observed.

Case 2: Energy transfer from porphyrin to the QD. Energy transfer from a Zinc porphyrin to a CdTe QD was recently demonstrated by Credi et. al. In that system there is significant overlap between the absorption of large 5.6 nm CdTe QDs and the emission of the porphyrin. This resulted in photosensitization of the luminescence of the CdTe which was detected by the presence of the soret band in the excitation spectrum. In contrast, there is minimal overlap between the porphyrin emission and QD absorption (shaded area in Fig. 1) in the system reported here and no sensitised emission of the QD is observed. (Excitation spectra of the QD emission in the presence of the low equivalents of porphyrin showed no evidence of energy transfer process.)

Case 3: Electron transfer processes. In light of the above it is more likely that we are observing photo-induced electron transfer involving either oxidation or reduction of the porphyrin (pathways b and c respectively).[62] Jhonsi et. al. reported quenching of CdTe (TGA capped) emission by a negatively charged free base porphyrin that was accompanied by sensitised emission of the porhyrin. However, the addition of the positively charged free base TMPyP resulted in quenching of the QD without any sensitised emission of the base and was attributed to electron transfer between the TMPyP free base porphyrin and the QD.[63] Our zinc porphyrin may be both readily oxidised or reduced {$E^o(P^{\bullet+}/P)$ = 1.18 V and $E^o(P/P^{\bullet-})$ = -0.85V}.[42] The redox properties of CdTe have been shown to be size-dependent and influenced by the nature of the capping ligand.[64] Using the measured oxidation potential for CdTe in the range from 2.95 nm to 4.08 nm,[64,65] we have estimated an oxidation potential of approximately +0.95 V, and a reduction potential of approximately -1.00 V for our 2.3 nm species.[66] The thermodynamic likelihood of reduction or oxidation of ZnTMPyP4 by photo-excited CdTe QD in a polar solvent can be

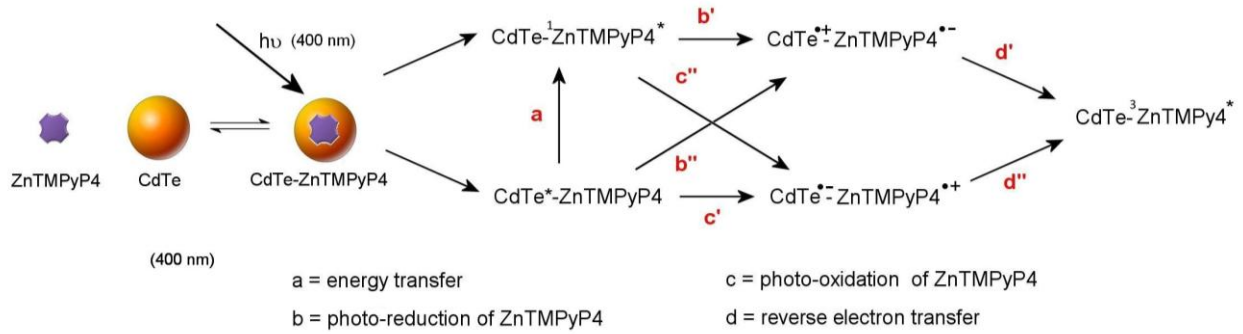

Scheme 2: Overview of the possible excited-state deactivation pathways for the CdTe-ZnTMPyP4 system

estimated from the approximated Rehm Weller equations Eq. 1 and Eq. 2, given below.

Eq. 1. $\Delta G^0 = E^o(CdTe^{\bullet+}/CdTe) - E^o(ZnTMPyP4/ZnTMPyP4^{\bullet-}) - h\nu$

Eq. 2. $\Delta G^0 = E^o(ZnTMPyP4^{\bullet+}/ZnTMPyP4) - E^o(CdTe/CdTe^{\bullet-}) - h\nu$

Where ΔG^0 is the Gibbs free energy, E^o are the standard potentials of donor and acceptor, hυ is the excited state energy of photo-excited QD, while electrostatic terms are neglected. Using these equations we obtain free energy values (ΔG^0) of -0.56 V for reduction of ZnTMPyP4 and -0.19 V for the oxidation of ZnTMPyP4.[67]

Electron transfer may also be considered starting with the photo-excited porphyrin singlet state. However, due to the lower excited state energy of ZnTMPyP4 (1.96 eV)[68] relative to CdTe, any photoinduced processes from the ZnTMPyP4 excited states would be expected to occur with a considerably lower driving force. Overall our 'approximated' Rehm Weller treatment indicates that the most likely electron transfer event is the reduction of the ZnTMPyP4 by the QD. It may be noted that the favourable energetics for the photoreduction of the porphyrin (process b') offers an explanation for the absence of porphyrin fluorescence. This may be contrasted with the reports for the phthalocyanine- 2.9 nm CdTe system reported by Nyokong and co-workers, where the photoreduction is energetically unfavourable and therefore fluorescence from the dye is observed.[60,61]

Finally we consider the nature of the long-lived species. While it is possible that this is the ZnTMPyP4 radical anion, we believe the ultimate fate of the excitation energy is the formation of the excited triplet state. If electron transfer (i.e. processes b or c) dominate then the triplet state will form by process d, which is expected to be efficient. The assignment of the long-lived species as the triplet state is consistent with the strong absorption band at ca. 480 nm. However, the porphyrin radical anion also shows strong absorption in this spectral region.[62] Therefore such an assignment of the triplet state is equivocal at the moment.

Conclusion

The properties of a donor-acceptor system comprising a ZnTMPyP4 porphyrin and CdTe QD have been studied in detail. Steady state measurements reveal a high binding affinity between the negatively charged QD (multiple COO- groups) and the positively charged porphyrin (+4). Mutual quenching is observed in the system. The surface area of the QD allows for multiple binding and quenching, of up to four porphyrin molecules. Furthermore, SAXS measurements revealed the formation of small CdTe-porphyrin assemblies in solution. Picosecond transient absorption measurements reveal ultrafast recovery (1.3 ps) of the CdTe excited state in the presence of a surface bound porphyrin. Critically, the depletion of the porphyrin ground state is found to occur over a correspondingly short timescale. This indicates the role of an exchange process in the ultrafast dynamics of the system. While energy transfer is possible, no fluorescence from the porphyrin is observed. This either means energy transfer does not occur or that an immediate additional quenching process takes place. Approximate treatment Rehm Weller equation using the known redox properties for porphyrin and estimated values for the QD suggests that electron transfer from the QD to the porphyrin is the most favoured process. The favourable driving force taken together with the fast time of the process leads us to believe that reduction of the porphyrin is occurring.

Further experiments to probe this would require transient monitoring in the 800-1000 nm region and we would hope to carry out such experiments in the near future. Indeed, as there is a known correlation between particle size and the rate of emission, future experiments will also consider the role of QD particle size in terms of both the new photophysical properties and the change in porphyrin occupancy due to changes in the surface area.

Acknowledgements

This publication has emanated from research conducted with the financial support of Science Foundation Ireland under Grant Numbers 07/IN.1/I1862 RFP/007/CHEF437 and 10/RFP/CAP2915, the EU for funded access to STFC (App 1110017) and start up funding from the School of Chemistry and Chemical Biology.

Experimental

CdTe QDs were synthesised using a modified method by Gaponik and co-workers.[2] $Cd(ClO_4)_2 \bullet 6H_2O$ and the stabiliser TGA were added to 150 mL degassed Millipore water in 1:1.4 ratio. The pH of the solution was adjusted to 11 by dropwise addition of a 2 M NaOH solution. H_2Te gas was generated by the

addition of 15 mL of H_2SO_4 to a known weight of Al_2Te_3 (molar ratio of 0.25 to Cd), which was then bubbled through the Cd/thiol solution. The resulting non-luminescent solution was then heated under reflux. Once the QDs reached the desired size, the reflux was stopped and different fractions were obtained via size-selective precipitation using isopropanol. The final samples were further purified on a Sephadex-G25 column. Solutions of known concentration of **ZnTMPyP4** were prepared using the literature value for the extinction coefficient at 436 nm $= 2.04 \times 10^5$ $dm^3 . mol^{-1} . cm^{-1}$.[69]

The SAXS measurements were performed on a SAXSess high-flux small-angle X-ray scattering instrument (Anton Paar, Austria), attached to a PW3830 X-ray generator (PANalytical) with a sealed-tube anode (Cu Kα wavelength of 0.1542 nm). The generator was operated at 40 kV and 50 mA. The SAXSess camera was equipped with a line collimator block and all measurements were performed at vacuum conditions for an intense and monochromatic primary beam with low background. A semitransparent beam stop was used to enable the measurements of an attenuated primary beam for the exact definition of the zero scattering vector and transmission correction. Vacuum-tight refillable quartz capillaries (1 mm diameter, sample volume ≤ 100 µL) were used in order to determine the size and shape of the w/o- quantum dots. All experiments were performed at room temperature. The 2-D scattered intensities were recorded on a CCD detector (Princeton Instruments) and were converted via SAXSQuant software (Anton Paar) to one dimensional scattering curves as a function of the magnitude of the scattering vector, where θ is the total scattering angle. All intensities were transmission-calibrated by normalizing the attenuated primary intensity at q = 0 to unity and were corrected the background scattering from the capillary and the solvent (H_2O). Data analysis employed the GIFT software by using the hard spheres, polydisperse model (PY, averaged structure factor). Detailed description of the data treatment is outlined in ESI Note S1.

UV-Vis absorption spectra were recorded at room temperature using a Cary 50 scanning spectrometer. Emission spectra were recorded using a Varian Cary Eclipse Fluorescence Spectrophotometer working in fluorescence mode. All samples were examined in a 1 cm quartz cell. The solvent used was Millipore water.

The samples for UV-vis transient absorption measurements were prepared in water as follows; a known volume of solution was dropped between two CaF_2 (25 mm diameter) windows (Crystan Ltd., UK), separated by a Teflon spacer of known length (typically 340 µm), in a demountable solution IR cell (Harrick Scientific Products Inc., New York). The picosecond transient absorption pump-probe experiments were carried out by using the high-sensitivity ULTRA apparatus at the Central Laser Facility of the Science & Technology Facilities Council in the Rutherford Appleton Laboratory.[70] All measurements were made at magic angle. Excitation pulse energy was monitored before each experiment and set to either 100 nJ (560 µJ/cm^2) or 5 nJ (28 µJ/cm^2) using a circular variable neutral density filter. In front of the monochromator, a 400 nm interference filter was placed in order to remove scatter from the excitation beam. During pump-probe experiments samples were rastered to minimize photodecomposition effects and to avoid eventual re-excitation. Samples were also frequently checked for decomposition by using standard UV-visible spectroscopy.

Notes and references

[a] *School of Chemistry and Chemical Biology, Centre for Synthesis and Chemical Biology, University College Dublin, Dublin 4, Fax: 353 1 716 1178; Tel: 353 1 716 2407; E-mail: susan.quinn@ucd.ie*
[b] *School of Chemistry ,Trinity College Dublin, Dublin 2, Ireland*
[c] *Central Laser Facility, Research Complex at Harwell, Science & Technology Facilities Council, Rutherford Appleton Laboratory, Didcot, Oxfordshire, OX11 0QX, UK*

† Electronic Supplementary Information (ESI) available: [**CdTe-TGA** characterisation, additional UV/vis plots for CdTe-**ZnTMPyP4** complex, Ps-TA spectra and kinetic fits at different pump energies, concentrations and binding ratios, note on redox calculations]. See DOI: 10.1039/b000000x/

1. U. Resch-Genger, M. Grabolle, S. Cavaliere-Jaricot, R. Nitschke, T. Nann *Nature Methods* 2008, **5**, 763-775.
2. J.-J. Peng, S.-P. Liu, L. Wang, Y.-Q. He *Spectrochimica Acta A* 2010, **75** 1571-1576; N. Gaponik, S. G. Hickey, D. Dorfs, A. L. Rogach, A. Eychmuller, *Small*, **6**, 1364-1378; F. Hetsch, X. Q. Xu, H. K. Wang, S. V. Kershaw, A. L. Rogach, *J. Phys. Chem. Lett.*, **2**, 1879-1887; A. L. Rogach, *Nano Today*, **6**, 355-365; A. L. Rogach, N. Gaponik, J. M. Lupton, C. Bertoni, D. E. Gallardo, S. Dunn, N. L. Pira, M. Paderi, P. Repetto, S. G. Romanov, C. O'Dwyer, C. M. S. Torres, A. Eychmuller, *Angew. Chemie Intl Ed.* 2008, 47, 6538-6549; J. Schafer, J. P. Mondia, R. Sharma, Z. H. Lu, A. S. Susha, A. L. Rogach, L. J. Wang, *Nano Letts.* 2008, **8**, 1709-1712.
3. P. Alivisatos, *Nature Biotechnology* 2004, **22**, 47-52.
4. T. M. Jovin, *Nature Biotechnology* 2003, **21**, 32-33.
5. K. Rajeshwar, N. R. de Tacconi, C. R. Chenthamarakshan, *Chem. Mat.* 2001, **13**, 2765-2782.
6. M. Achermann, M. A. Petruska, D. D. Koleske, M. H. Crawford, V. I. Klimov, Nano Letters 2006, **6**, 1396-1400.
7. J. Liu, T. Tanaka, K. Sivula, A. P. Alivisatos, J. M. J. Frechet, *J. Am. Chem. Soc.*, 2004, **126**, 6550-6551.
8. S. Chanyawadee, R. T. Harley, D. Taylor, M. Henini, A. S. Susha, A. L. Rogach, P. G. Lagoudakis, *App. Phys. Letts.*, 2009, **94**, 233502.
9. Q. J. Sun, Y. A. Wang, L. S. Li, D. Y. Wang, T. Zhu, J. Xu, C. H. Yang, Y. F. Li, *Nature Photonics*, 2007, **1**, 717-722.
10. I. Nabiev, S. Mitchell, A. Davies, Y. Williams, D. Kelleher, R. Moore, Y. K. Gun'ko, S. Byrne, Y. P. Rakovich, J. F. Donegan, A. Sukhanova, J. Conroy, D. Cottell, N. Gaponik, A. Rogach, Y. Volkov, Nano Letters 2007, **7**, 3452-3461; S. J. Byrne, S. A. Corr, T. Y. Rakovich, Y. K. Gun'ko, Y. P. Rakovich, J. F. Donegan, S. Mitchell, Y. Volkov, *J. Mat. Chem.*, 2006, **16**, 2896-2902; S. J. Byrne, B. le Bon, S. A. Corr, M. Stefanko, C. O'Connor, Y. K. Gun'ko, Y. P. Rakovich, J. F. Donegan, Y. Williams, Y. Volkov, P. Evans, *Chemmedchem.*, 2007, **2**, 183-186.
11. M. P. Moloney, Y. K. Gun'ko, J. M. Kelly, Chemical Communications 2007, 3900; J. E. Govan, E. Jan, A. Querejeta, N. A. Kotov, Y. K. Gun'ko, *Chem. Comm.*, 2010, **46**, 6072-6074; S. A. Gallagher, M. P. Moloney, M. Wojdyla, S. J. Quinn, J. M. Kelly, Y. K. Gun'ko, *J. Mat. Chem.*, 2010, **20**, 8350-8355.
12. C. Wadia, A. P. Alivisatos, D. M. Kammen *Environ. Sci. Technol.*, 2009, **43**, 2072–2077.
13. I. J. Kramer and E.H. Sargent, *ACS Nano*, 2011, **5**, 8506–8514
14. A. J. Nozik Nano Lett., 2010, **10**, 2735–2741.
15. P. V. Kamat, K. Tvrdy, D. R. Baker, J.G. Radich Chem. Rev., 2010, **110**, 6664–6688.
16. E. Holder, N. Tessler, A. L. Rogach *J. Mater. Chem.*, 2008, **18**, 1064-1078.
17. A. L. Rogach, A. Kornowski, M. Gao, A. Eychmüller and H. Weller, *J. Phys. Chem. B.*, 1999, **103**, 3065-3069; N. Gaponik, D. V. Talapin, A. L. Rogach, K. Hoppe, E. V. Shevchenko, A. Kornowski, A. Eychmüller and H. Weller, *J. Phys. Chem. B.*, 2002, **106**, 7177-7185; A. L. Rogach, T. Franzl, T. A. Klar, J. Feldmann, N. Gaponik, V.

Lesnyak, A. Shavel, A. Eychmuller, Y. P. Rakovich, J. F. Donegan, *J. Phys. Chem. C.*, 2007, **111**, 14628-14637.
18. Miyawaki, A.; Llopis, J.; Heim, R.; McCaffery, J. M.; Adams, J. A.; Ikura, M.; Tsien, R. Y. *Nature* 1997, **388**, 882-887.
19. Medintz, I. L.; Clapp, A. R.; Mattoussi, H.; Goldman, E. R.; Fisher, B.; Mauro, J. M. *Nat. Mater.*, 2003, **2**, 630-638
20. D. M. Willard, T. Mutschler, M. Yu, J. Jung, A. Van Orden, *Anal. Bioanal. Chem.*, 2006, **384**, 564-571.
21. M. Achermann, M. A. Petruska, S. Kos, D. L. Smith, D. D. Koleske, V. I. Klimov, *Nature*, 2004, **429**, 642-646.
22. N.Cicek, S. Nizamoglu, T. Ozel, E. Mutlugun, D. U. Karatay, V. Lesnyak, T. Otto, N. Gaponik, A. Eychmüller, H. V. Demir, *Appl. Phys. Lett.*, 2009, **94**, 061105.
23. S. Chanyawadee, P. G. Lagoudakis, R. T. Harley, M. D. B. Charlton, D. V. Talapin, H.W. Huang, C.H. Lin, *Adv. Mater.* 2010, **22**, 602-606.
24. Y. Yan, G. Chen, P. G. Van Patten *J. Phys. Chem. C.*, 2011, **115**, 22717–22728.
25. S.Rawalekar, S. Kaniyankandy, S.Verma, H.N. Ghosh *J. Phys. Chem. C.*, 2010, **114**, 1460–1466.
26. M. S. Miguel A. Correa-Duarte, L. M. Liz-Marz´, A. Douhal *J. Photochem. Photobiol. A* 2008, **196**, 51–58E.
27. T. S. Balaban *Acc. Chem. Res.* 2005, **38**, 612-623.
28. M. C.O'Sullivan, J. K. Sprafke, D. V.Kondratuk, C. Rinfray, T. D.W. Claridge, A. Saywell, M. O. Blunt, J. N. O'Shea, P. H. Beton, M. Malfois, H. L. Anderson *Nature* 2011, **469**,72-75,
29. X. Feng, L. Liu, Y.Honsho, A.Saeki, S. Seki, S. Irle, Y. Dong, A. Nagai, D. Jiang *Angew. Chem. Int. Ed.* 2012, *51*, 2618 –2622
30. J. Bhuyan S. Sarkar *Cryst. Growth Des*. 2011, **11**, 5410–5414.
31. Q.Wang, W. M. Campbell, E. E. Bonfantani, K. W. Jolley, D. L. Officer, P. J. Walsh, K. Gordon, R. Humphry-Baker, M. K. Nazeeruddin, M. Gratzel *J. Phys. Chem. B* 2005, **109**, 15397-15409.
32. M. V. Martínez-Díaz , G. de la Torre T, Torres *Chem. Commun.*, 2010, **46**, 7090-7108.
33. N. K. Subbaiyan, E. Maligaspe, F. D'Souza Appl. Mater. Interfaces 2011, **3**, 2368–2376.
34. M. G. Waltera, A. B. Rudineb, C. C. Wamser *J. Porphyrins Phthalocyanines* 2010, **14**, 759–792.
35. E. Kikuchi, S. Kitada, A. Ohno, S. Aramaki, S. Maenosono *Appl. Phys. Lett.* 2008, **92**, 173307.
36. K. Akatsuka, Y. Ebina, Muramatsu, T. Sato, H. Hester, D. Kumaresan, R. H. Schmehl, T.Sasaki, M.-a. Haga *Langmuir*, 2007, **23**, 6730–6736.
37. J. M. Kelly, M. J. Murphy, D. J. McConnell, C. OhUigin, *Nucl. Acids Res.* 1985, **13**, 167-184.
38. A. J. Bhattacharjee, K. Ahluwalia,. Taylor, O. Jin, J. M. Nicoludis, R. Buscaglia, J. B. Chaires, D. J. P. Kornfilt, D. G. S. Marquardt, L. A. Yatsunyk, *Biochimie* 2011, **93**, 1297-1309.
39. S. Moeno, M. Idowu, T. Nyokong *Inorg. Chimica Acta* 2008, **361**, 2950–2956.
40. M. A. Jhonsi, R. Renganathan *J. Colloid and Interface Sci.* 2010, **344**, 596–602.
41. M. Amelia, A.Credi *Inorg. Chimica Acta*, 2012, **381**, 247-250.
42. K. Kalyanasundaram, *J. Phys. Chem.*, 1982, **86**, 5163-5169.
43. W. W. Yu, L. Qu, W. Guo, X. Peng, *Chem. Mat.* 2003, **15**, 2854-2860.
44. Based on the surface area of 16.6 nm^2 calculated for a 2.3 nm spherical particle and the thiol foot print of 0.22 nm^2 the maximum number of surface TGA molecules was estimated to be approximately 75.[45]
45. G.H. Woehrle, L.O. Brown, J. E. Hutchison *J. Am. Chem. Soc.* 2005, **127**, 2172-2183.
46. T. Uematsu,T. Waki,T. Torimoto, S. Kuwabata *J. Phys. Chem. C.*, 2009, **113**, 21621–21628.
47. C.D. Putnam, M. Hammel, G.L. Hura, J. A., Tainer, 2007. *Quart. Rev. Biophysics*, 2007, **40**, 191–285.
48. J. Brunner-Popela, O. Glatter, *J. Appl. Crys.*, 1997, **30**, 431-442.
49. O. Glatter, *J. Appl. Crys.*, 1977, **10**, 415-421.
50. T.-L. Lin, U. Jeng, C.-S. Tsao, W.-J. Liu, T. Canteenwala, L. Y. Chiang J. Phys. Chem. B 2004, **108**, 14884-14888.
51. B. D'Aguanno R., Klein *Light Scattering. Principles and Development*, Oxford University Press, Oxford, 1996.
52. J. P. Hansen, I. R. McDonald, *Theory of Simple Liquids* Academic Press, Burlington, 2006.
53. J.-P. Hansen, J. B. Hayter, *Mol. Phys.*, 1982, **46**, 651-656.
54. G. Fritz, A. Bergmann, O. Glatter, Evaluation of small-angle scattering data of charged particles using the generalized indirect Fourier transformation technique, AIP, 2000.
55. S. Connolly, D.Fitzmaurice *Adv. Mater.* 1999, **11**, 1202-1205.
56. M. Enescu, K. Steenkeste, F. Tfibel, M.-P.Fontaine-Aupart *Phys. Chem. Chem. Phys.*, 2002, **4**, 6092–6099.
57. J. A. McGuire, J. Joo, J. M. Pietyrga, R. D. Schaller, V. I. Klimov *Acc. Chem. Res.*, 2008, **41**, 1810-1819; C. Burda, S. Link, T. C. Green, M. A. El-Sayed *J. Phys. Chem. B.* 1999, **103**, 10775-10780.
58. A. R. Clapp, I. L. Medintz, H. T. Uyeda, B.R. Fisher, E. R. Goldman, M. G. Bawendi, H. Mattoussi *J. Am. Chem. Soc.*, 2005, **127**,18212–18221.
59. S. Dayal, R. Krolicki,Y. Lou, Y. Qui, J.C. Berlin, M.E. Kenney, C. Burda *Appl. Phys. B:* 2006, **84**, 309-315.
60. M. Idowu, J. –Y. Chenab, T. Nyokong, *New J. Chem.*, 2008, **32**, 290–296.
61. S. Moeno, T. Nyokong *Polyhedron* 2008, **27**, 1953–1958.
62. P. Neta, J. Phys. Chem., 1981, 85, 3678-3684,
63. M. A. Jhonsi, R. Renganathan, *J. Colloid Interface Sci.* 2010, **344**, 596–602.
64. S. K. Poznyak, N. P. Osipovich, A. Shavel, D.V. Talapin, M. Gao, A. Eychmuller,. N. Gaponik *J. Phys. Chem. B.*, 2005, **109**, 1094 1100
65. S. Moeno, M. Idowu, M.; Nyokong, T. *Inorg. Chimica Acta*, 2008, **361**, 2950-2956.
66. Based on a linear extrapolation of data for a number particle sizes by Moeno et al (ref 62,63) CdTe data recorded vs. Ag/AgCl, corrected to SHE by +0.2 V.
67. For reduction of the porphyrin: $\Delta G = E^o(CdTe^{\bullet+}/CdTe) - E^o(ZnTMPyP4/ZnTMPyP4^{\bullet-})$- hν = 0.95 V –(–0.85V) – 2.37 V = – 0.57 V and for oxidation of the porphyrin: $\Delta G = E^o(ZnTMPyP4^{\bullet+}/ZnTMPyP4) - E^o(CDTe/CdTe^{\bullet-})$ –hν = 1.18V –(–1.00 V) – 2.37 V = – 0.19 V.
68. Energy assumed to be 1.96 eV based on a wavelength of 632 nm for the overlap of the absorption and fluorescence bands of the QD-bound species.
69. R. F. Pasternack, R. A Brigandi, M. J. Abrams, A. P. Williams, E. J. Gibbs, *Inorg. Chem.*, 1990, **29**, 4483-4486.
70. G. M. Greetham, P. Burgos, Q. Cao, I. P. Clark, P. Codd, R. C. Farrow, M. W. George, M. Kogimtzis, P. Matousek, A. W. Parker, M. R. Pollard, D. A. Robinson, Z.-J. Xin, M. Towrie Appl.Spec. 2010, 64, 1311-1319.